Molecular beams of neutron-rich cerium isotopes for Coulomb-excitation experiments

June 1, 2016

L. P. Gaffney[1], J. Ballof[2], P. A. Butler[3], D. M. Cox[4], A. B. Garnsworthy[5],
P. E. Garrett[6], L. Harkness-Brennan[3], D. T. Joss[3], Th. Kröll[7], P. Napiorkowski[8],
D. O'Donnell[1], J. Pakarinen[4], R. D. Page[3], P. Papadakis[4], J. P. Ramos[2], M. Scheck[1],
G. S. Simpson[9], J. Smallcombe[5], J. F. Smith[1], T. Stora[2], J. L. Wood[10],
K. Wrzosek-Lipska[8], M. Zielińska[11]

[1]*University of the West of Scotland, U.K.* | [2]*CERN-ISOLDE, Switzerland* | [3]*University of Liverpool, U.K.* | [4]*University of Jyväskylä and Helsinki Institute of Physics, Finland* | [5]*TRIUMF, Canada* | [6]*University of Guelph, Canada* | [7]*TU Darmstadt, Germany* | [8]*HIL, University of Warsaw, Poland* | [9]*LPSC Grenoble, France* | [10]*Georgia Institute of Technology, U.S.A.* | [11]*CEA-Saclay, France*

Spokespersons: L. P. Gaffney [Liam.Gaffney@uws.ac.uk]
Contact person: T. Stora [thierry.stora@cern.ch]

Abstract: This letter of intent proposes the development of intense and pure post-accelerated cerium beams at HIE-ISOLDE in order to perform Coulomb-excitation measurements. The aim of the consequent experiments is to determine, simultaneously, $\rho^2(0_2^+ \to 0_1^+)$ values and the degree of octupole collectivity in $N \simeq 88, 90$ nuclei via the measurement of $B(E2; 0_2^+ \to 2_1^+)$ and $B(E3; 0_1^+ \to 3_1^-)$ values, respectively. The most promising route to this development is via the extraction of molecular beams which will suppress contamination from caesium isobars and which can then be later broken up in REX-EBIS. Fluorides appear to be the most suitable compound and the highest yields are likely to come from uranium-carbide or thorium-oxide targets. Yield measurements are required for the neutron-rich cerium isotopes, ^{146,148}Ce, to assess the feasibility and beam-time requirements for the Coulomb-excitation experiments.

Requested shifts: 3 shifts for yield measurements.

1

1 Physics Case

Low-lying 0^+ ***states:*** Electromagnetic properties of non-yrast states at low energy and low spin are required in order to understand the collective structures that dominate in the ground states of atomic nuclei. There is particularly important when different collective modes compete with each other, either in terms of vibrational and rotational degrees of freedom or coexisting shapes [1]. In even-even nuclei, low-lying excited 0^+ states are often key signatures of shape coexistence [1]. However, the β-vibrational mode in deformed nuclei, described by Bohr and Mottelson, also gives rise to excited 0^+ states and detailed spectroscopy, especially determination of electromagnetic properties, can help to distinguish between them. It has long been debated as to whether the harmonic-vibrator description of nuclei is robust though, given the lack of clear candidates across the nuclear chart. Studies of the cadmium isotopes [2, 3], often considered the best examples of harmonic vibrators, reveals the breakdown of this description on the basis of detailed measurements of electromagnetic properties. That work highlights the need to base the collective description of nuclear phenomena on much more than just the interpretation of level energies. A particularly useful observable in this case is the $\rho^2(0_i^+ \rightarrow 0_1^+)$ value, which indicates a mixing between configurations with different deformations [4].

In many cases around $N = 90$, excited 0^+ states have long been attributed to β vibrations but doubt has been cast on these assignments [5]. However, there is evidence to suggest that the description of shape coexistence is better suited to $N \approx 90$ nuclei [6, 7]. Along the $N = 90$ isotopic chain, the stable isotopes ^{150}Nd, ^{152}Sm and, in particular, ^{154}Gd have been subject to much experimental scrutiny due to both the suggestion of β vibrations and the critical-point description of Iachello within the Interacting Boson Approximation (IBA) [8]. Recent beyond-mean-field (BMF) calculations in this region [9] show that a quantitive approach to resolve this ambiguity is possible. They reveal that the deformation of excited 0^+ states in the $N = 90$ isotones differ from their ground states [9]. This hints more towards shape coexistence where the $E0$ strength is an indication of the mixing between configurations. On the other hand, systematic calculations within the dynamic pairing-plus-quadrupole model (DPPQM) [10] have recently lead to the conclusion that the description of a β band is a good one, going as far as to rule out shape coexistence [11]. In the $N = 90$ chain, data for the transition strengths is still missing, particularly $\rho^2(0_2^+ \rightarrow 0_1^+)$ values and especially beyond the stable isotopes. The next even-Z isotone on the lighter side of this sequence, ^{148}Ce, is radioactive and therefore much less studied. The energy systematics of 0_2^+ states in this region are shown in the top part of Fig. 1, where a minimum is approached at $N = 90$ for Sm, Nd and Ce. The two key components in determining $\rho^2(0_2^+ \rightarrow 0_1^+)$ are the $E0$ branching ratio and the lifetime of the 0_2^+ state. In the majority of even-even nuclei, the 2_1^+ state lies below the 0_2^+ state allowing for a lifetime measurement via $B(E2; 0_2^+ \rightarrow 2_1^+)$, given that the branching ratio is known. With this in mind, complementary experiments at TRIUMF laboratory, Canada, have been proposed by the same collaboration and accepted with high priority to give precise measurements of $E0/E2$ branching ratios in the $N = 88, 90$ nuclei, ^{146,148}Ce [13]. This paves the way for Coulomb-excitation experiments to determine the $B(E2; 0_2^+ \rightarrow 2_1^+)$ values, extending our understanding of ρ^2 values in this region.
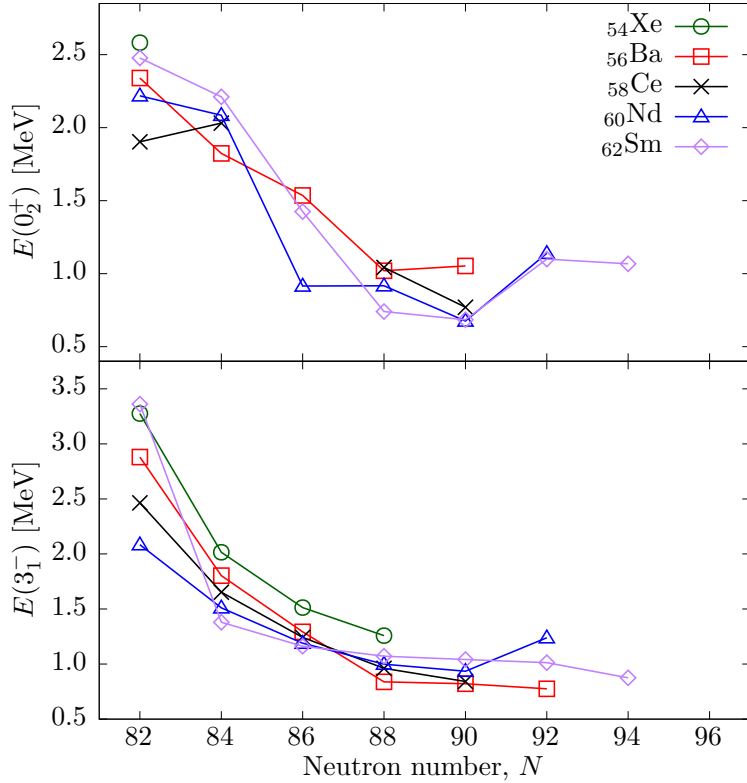
Figure 1: Excitation energy systematics of the first-excited 0^+ (top) and 3^- (bottom) states in the $N = 90$ region. Both the 3_1^- and 0_1^+ energies appear to minimise around $N = 88, 90$. Data is taken from NNDC [12].

Octupole collectivity: The structure of transitional nuclei such as ^{148}Ce and its neighbours cannot be described by a single simplified model. However, it is rare that there are multiple collective processes competing at such low-energy. Octupole correlations have been noted around $Z = 56, N = 88$ for some time [14–16] and low-lying negative-parity bands are known in the heavy cerium isotopes. The excitation energies of the lowest-lying 3^- states in this region are plotted in Figure 1, where it is shown that they approach a minimum around the "octupole magic number", $N = 88$. These states also lie very close in energy to the 0_2^+ states, giving rise to a complex mixture of quadrupole and octupole degrees of freedom that is so far unresolved. Studying the electromagnetic properties of excited states in nuclei with octupole correlations is crucial to understanding such a subtle interplay [17]. New calculations going beyond the mean-field are proving to be the most reliable way of making predictions about octupole states in the actinide region [9, 18, 19] and now also in the lanthanide region [20]. The most recent global analysis of ground-state properties using covariant density functional theory shows how important ^{148}Ce is in this context [21]. In these calculations, a minimum is predicted in the potential energy surface at $\beta_3 = 0.125$ for ^{148}Ce, with a gain in binding energy of more than 700 keV due to the octupole deformation, the largest in the region. In order to test these predictions rigorously, systematic and precise data on $E3$ matrix elements is required in addition to the single, low-precision data point of ^{144}Ba in this region [22].

Studying octupole collectivity with Coulomb excitation at ISOLDE has been established with experiments in the actinide region [23] and the first steps in the lanthanide region are proposed with ^{142,144}Ba [24]. A recent experiment at the CARIBU facility at Argonne National Laboratory has provided the first measurement of a $B(E3; 0_1^+ \rightarrow 3_1^-)$ value in

this region, albeit with a very large uncertainty [22]. Experiments at HIE-ISOLDE have the potential to provide much cleaner and more intense beams than what is currently possible with CARIBU, especially in the case of cerium isotopes, the beams of which are so far unexplored at ISOLDE. Cleanliness of the beams is crucial in order to gather the high-quality γ-ray spectra required for precise measurements of Coulomb-excitation cross sections.

2   Planned experiments

Experimental technique: Coulomb excitation (Coulex) at "safe" energies is an excellent tool to measure transition strengths connecting low-lying states, where "safe" implies that the nuclear surfaces of the interacting nuclei are separated by a minimum distance of 5 fm. To ensure the safe condition is met, a balance has to be struck between beam energy and the maximum centre-of-mass (CoM) scattering angle. For beam energies of up to 5.0 MeV/u, soon to be available at HIE-ISOLDE, only the forward CoM angles $< 90°$ satisfy the safe energy criterion. If multiple-step Coulomb excitation is desired, as is the case here, the highest CoM angles are required and a beam energy of 4.0 MeV/u has been determined as the optimum value for these studies.

The Miniball Ge-detector array [25] will be used to detect the de-excitation γ rays following Coulomb excitation. This will be coupled to the new SPEDE chamber for Coulomb-excitation experiments, which adds a cooled Si detector in the upstream of the target position for conversion electron detection [26]. A double-sided silicon strip detector (DSSSD) in the forward laboratory angles will be used to detect the scattered projectiles and recoiling target nuclei. The granularity of the Miniball Ge detectors, SPEDE and the CD detector allows for Doppler correction to be applied to γ rays and electrons emitted in flight. The particle-γ-ray coincidence intensities can then be related to the excitation cross-sections in order to extract nuclear-structure information, such as transition strengths and quadrupole moments. The population of the 0_2^+ can be inferred from a combination of the $0_2^+ \rightarrow 2_1^+$ $E2$ γ-ray intensity and the $0_2^+ \rightarrow 0_1^+$ $E0$ conversion electron intensity, detected in SPEDE. The $E0/E2$ branching ratio is expected to be $\approx 1\%$ and will be measured to high precision in the upcoming β-decay experiments at TRIUMF. All of the data combined provide stringent constraints on the fit and reduces the uncertainties.

Cross sections and beam-time estimates: It is planned to measure two quantities simultaneously in these experiments, namely $B(E3; 3_1^- \rightarrow 0_1^+)$ and $B(E2; 0_2^+ \rightarrow 2_1^+)$, in ^{146,148}Ce. Calculations have been performed with the Coulomb-excitation code, GOSIA [27, 28], using an estimated set of electromagnetic matrix elements and typical Miniball geometries for scattering [25]. A ^{60}Ni target of 2 mg/cm^2 in thickness is chosen in order to cleanly detect the recoils in the forward-facing CD detector without ambiguity in the energy vs. angle kinematics between the angles of 28° to 58° in the laboratory frame. Normalisation of the data is expected to be provided by the precise lifetimes of the 2_1^+ and 4_1^+ states, which will also be remeasured in the upcoming TRIUMF β-decay experiments [13]. It is therefore advantageous that the ^{60}Ni target has a small excitation cross section, keeping the γ-ray spectra free from target contamination. In turn, this also means that beam purity does not have to be 100% and instead, depending on the energy

Table 1: Summary of the required beam-time for planned Coulomb-excitation experiments. Experimental details are given in the text. Cross sections are integrated over both scattering angle and energy through the target. Matrix elements used to calculate cross-sections come from measured values [12] or theoretical predictions [18], extrapolated to higher spins using the rigid rotor model. The integrated number of beam particles, Q_b, required to achieve at least 500 γ-ray counts in the relevant depopulating transitions and the corresponding number of shifts required for a production yield of 1×10^6 ions/μC are shown. We assume a proton current of 2 μA and a post-acceleration efficiency of 5%.

Isotope	I^π	$E(I^\pi)$	σ [fm^2]	$E_\gamma(I^\pi \to 2_1^+)$	ϵ_γ	Q_b	# shifts
^{146}Ce	0_2^+	1043 keV	870	785 keV	6.9%	5×10^9	2
	3_1^-	961 keV	19	702 keV	7.3%	3×10^{11}	90
^{148}Ce	0_2^+	770 keV	2400	612 keV	7.9%	18×10^8	1
	3_1^-	841 keV	40	683 keV	7.4%	13×10^{10}	46

of the γ rays in the contaminant species, would be acceptable down to 50%.

Estimates of the required integrated beam current to achieve $\leq 10\%$ uncertainty on these quantities is presented in Table 1. It is clear that the physics aims related to low-lying 0^+ states can be achieved with relatively little beam time, even allowing for lower than predicted production yields. However, the more challenging part of the experiment comes with the determination of $B(E3)$ values to study octupole collectivity in these nuclei. The cross sections for populating the 3_1^- states are a factor of ≈ 50 lower than for the 0_2^+ states, leading to similar factors in the required beam time or number of γ-ray counts in the de-excitation spectrum. The benchmark here will be to achieve clean cerium beams delivered to Miniball with a minimum intensity of 2×10^5 pps for ^{148}Ce, allowing for a measurement of the $B(E3; 3_1^- \to 0_1^+)$ value in less than one week of beam time.

3   Beam development

Cerium beams have never been tested at ISOLDE before and as such, production yields do not exist in the ISOLDE yield database [29], except for the molecular beam of ^{133}Ce^{16}O$_2^+$ [30]. This molecular beam measurement originates from a Ta target of 122 g/cm^2 thickness with plasma ion source and the yield is 1.9×10^6 ions/μC. In order to determine if the experiments outlined in Section 2 are feasible, accurate production yields of neutron-rich cerium isotopes must be determined, along with ionisation and extraction efficiencies. An online measurement dedicated to determining the extracted yields, which gives the product of all factors and can be directly compared to the experimental conditions, is required.

Ionisation and extraction: Ionisation and extraction of cerium beams from ISOL targets can be achieved using a hot-surface ion source. Selectivity with such ion sources is very low, however, and at these masses caesium would cause large isobaric contamination.

It is proposed to use the molecular side-band method employed already for Ce [30], ionising in the new and advanced Versatile Arc-Discharge Ion Source (VADIS) [31]. Extraction of molecular beams in this way, the so-called chemical evaporation technique, has been proven using reactive gases to form volatile compounds of fluorides and oxides [32, 33]. The molecular beam can later be broken up in EBIS during the charge-breeding stage of the post-accelerator, as was done for ^{70}Se [34]. The latter step has the benefit of removing contamination from atomic ions at the same mass as the molecular compound.

The selection of the correct molecular compounds is crucial to optimise the yield and selectivity. The original cerium from ISOLDE was an oxide compound, CeO_2 [30], which has a melting point of 2450 K. In the other stable binary oxide compound of cerium, Ce_2O_3, this is higher at 2670 K. No binary compound of caesium, the most likely contaminant, and oxygen is known to be stable in these ratios. Other strongly produced oxides in the region are likely to be BaO and La_2O_3, meaning that the mass of $^{146,148}Ce^{16}O_2$ is potentially free from contamination. Melting points as high of these however, would likely be prohibitive for extraction.

In 2007, fluorination and molecular extraction was demonstrated at REX-ISOLDE. Barium fluoride, BaF, with a melting point of 1641 K was successfully extracted from a UC_x target (#359) coupled to a surface ion source and Coulomb-excitation measurements were performed on ^{140,142}Ba [35]. Cerium-flouride binary compounds that are known to be stable are CeF_3 and CeF_4, with melting points of 1733 K and 923 K, respectively, much lower than cerium oxide. At these masses, one would also expect LaF_3, the only stable fluoride of lanthanum, but not contamination from caesium or barium compounds. The lower melting point would appear to favour fluorides over oxides, but two known cerium-fluoride compounds exist. Their relative production in the hot target environment is unknown.

Production yields: It is proposed to use the standard UC_x target, which allows for fluorination or oxidisation with CF_2 or O_2 gas, respectively. In the case of oxides, a UO_2 or ThO_2 target may also be suitable to provide the oxygen by in-situ reduction of the target material. Production of ^{146,148}Ce from these targets would come mostly from proton-induced fission and uranium targets are likely to give the largest yields, sufficient enough to perform the measurement. However, the efficiency of the molecular extraction remains unknown. Yield measurements of cerium-fluoride compounds, $^{146,148}Ce^{19}F_x$, are required to determine their relative production and the level of contamination. In addition, the efficiency and stability of fluorination of the targets must be investigated, since up to seven days of beam time will be required to complete the physics aims of the experiment.

Summary of requested shifts: We request **3 shifts** to test fluorination of UC_2 target and measure yields of $^{146,148}CeF_x$.

References

[1] K. Heyde and J. L. Wood, Rev. Mod. Phys. **83**, 1467 (2011).

[2] P. E. Garrett, K. L. Green, and J. L. Wood, Phys. Rev. C **78**, 044307 (2008).

[3] P. E. Garrett and J. L. Wood, J. Phys. G Nucl. Part. Phys. **37**, 064028 (2010).

[4] J. L. Wood, E. Zganjar, C. De Coster, and K. Heyde, Nucl. Phys. A **651**, 323 (1999).

[5] J. F. Sharpey-Schafer et al., Eur. Phys. J. A **47**, 5 (2011).

[6] W. Kulp et al., Phys. Rev. C **77**, 061301 (2008).

[7] P. E. Garrett et al., Phys. Rev. Lett. **103**, 1 (2009).

[8] F. Iachello, Phys. Rev. Lett. **87**, 052502 (2001).

[9] Z. P. Li, T. Nikšić, and D. Vretenar, J. Phys. G Nucl. Part. Phys. **43**, 024005 (2016).

[10] K. Kumar and M. Baranger, Nucl. Phys. A **110**, 529 (1968).

[11] J. B. Gupta and J. H. Hamilton, Eur. Phys. J. A **51**, 151 (2015).

[12] J. Tuli, Evaluated Nuclear Structure Data File (ENSDF), 2012.

[13] L. P. Gaffney et al., Propososal to TRIUMF EEC *"Spectroscopy of negative-parity and excited 0^+ states in neutron-rich cerium isotopes"*, S1626 (2015).

[14] G. A. Leander et al., Nucl. Phys. A **388**, 452 (1982).

[15] P. A. Butler and W. Nazarewicz, Nucl. Phys. A **533**, 249 (1991).

[16] P. A. Butler and W. Nazarewicz, Rev. Mod. Phys. **68**, 349 (1996).

[17] L. M. Robledo and P. A. Butler, Phys. Rev. C **88**, 051302 (2013).

[18] L. M. Robledo and G. F. Bertsch, Phys. Rev. C **84**, 54302 (2011).

[19] J. M. Yao, E. F. Zhou, and Z. P. Li, Phys. Rev. C **92**, 041304 (2015).

[20] R. N. Bernard, L. M. Robledo, and T. R. Rodríguez, arXiv:1604.06706 (2016).

[21] S. E. Agbemava, A. V. Afanasjev, and P. Ring, Phys. Rev. C **93**, 044304 (2016).

[22] B. Bucher et al., Phys. Rev. Lett. **116**, 112503 (2016).

[23] L. P. Gaffney et al., Nature **497**, 199 (2013).

[24] M. Scheck et al., "Determination of the $B(E3, 0^+ \rightarrow 3^-)$ strength in the octupole correlated nuclei ^{142,144}Ba using Coulomb excitation", CERN-INTC **047**, 348 (2012).

[25] N. Warr et al., Eur. Phys. J. A **49**, 40 (2013).

[26] P. Papadakis et al., The SPEDE Spectrometer: Combined In-Beam γ-ray and Conversion Electron Spectroscopy with Radioactive Ion Beams, in *ARIS2014 Conf. Proc.*, volume 6, page 030023, JPS Japan, 2015.

[27] T. Czosnyka, D. Cline, and C. Y. Wu, Bull. Am. Phys. Soc. **28**, 745 (1983).

[28] D. Cline et al., *Gosia User Manual for Simulation and Analysis of Coulomb Excitation Experiments*, `http://www.pas.rochester.edu/$\sim$cline/Gosia/Gosia_Manual_20120510.pdf`, Rochester, NY, US, 2012.

[29] ISOLDE Yield Database.

[30] H.-J. Kluge, *Isolde Users' Guide*, CERN, Geneva, 1986.

[31] L. Penescu, R. Catherall, J. Lettry, and T. Stora, Rev. Sci. Inst. **81**, 02A906 (2010).

[32] R. Eder et al., Nucl. Instrum. Meth. B **62**, 535 (1992).

[33] U. Köster et al., Eur. Phys. J. Spec. Top. **150**, 285 (2007).

[34] A. M. Hurst et al., Phys. Rev. Lett. **98**, 072501 (2007).

[35] C. Bauer et al., Phys. Rev. C **86**, 034310 (2012).

Appendix

DESCRIPTION OF THE PROPOSED EXPERIMENT

The experimental setup comprises: (*name the fixed-ISOLDE installations, as well as flexible elements of the experiment*)

Part of the	Availability	Design and manufacturing
(if relevant, name fixed ISOLDE installation: MINIBALL + only CD, MINIBALL + T-REX)	☒ Existing	☒ To be used without any modification
[Part 1 of experiment/ equipment]	☐ Existing	☐ To be used without any modification ☐ To be modified
	☐ New	☐ Standard equipment supplied by a manufacturer ☐ CERN/collaboration responsible for the design and/or manufacturing
[Part 2 of experiment/ equipment]	☐ Existing	☐ To be used without any modification ☐ To be modified
	☐ New	☐ Standard equipment supplied by a manufacturer ☐ CERN/collaboration responsible for the design and/or manufacturing
[insert lines if needed]		

HAZARDS GENERATED BY THE EXPERIMENT (if using fixed installation:) Hazards named in the document relevant for the fixed [MINIBALL + only CD, MINIBALL + T-REX] installation.

Additional hazards:

Hazards	[Part 1 of experiment/ equipment]	[Part 2 of experiment/ equipment]	[Part 3 of experiment/ equipment]
Thermodynamic and fluidic			
Pressure	[pressure][Bar], [volume][l]		
Vacuum			
Temperature	[temperature] [K]		
Heat transfer			
Thermal properties of materials			
Cryogenic fluid	[fluid], [pressure][Bar], [volume][l]		
Electrical and electromagnetic			
Electricity	[voltage] [V], [current][A]		

Static electricity			
Magnetic field	[magnetic field] [T]		
Batteries	☐		
Capacitors	☐		
Ionizing radiation			
Target material [material]			
Beam particle type (e, p, ions, etc)			
Beam intensity			
Beam energy			
Cooling liquids	[liquid]		
Gases	[gas]		
Calibration sources:	☐		
• Open source	☐		
• Sealed source	☐ [ISO standard]		
• Isotope			
• Activity			
Use of activated material:			
• Description	☐		
• Dose rate on contact and in 10 cm distance	[dose][mSV]		
• Isotope			
• Activity			
Non-ionizing radiation			
Laser			
UV light			
Microwaves (300MHz-30 GHz)			
Radiofrequency (1-300 MHz)			
Chemical			
Toxic	[chemical agent], [quantity]		
Harmful	[chem. agent], [quant.]		
CMR (carcinogens, mutagens and substances toxic to reproduction)	[chem. agent], [quant.]		
Corrosive	[chem. agent], [quant.]		
Irritant	[chem. agent], [quant.]		
Flammable	[chem. agent], [quant.]		
Oxidizing	[chem. agent], [quant.]		
Explosiveness	[chem. agent], [quant.]		
Asphyxiant	[chem. agent], [quant.]		

Dangerous for the environment	[chem. agent], [quant.]		
Mechanical			
Physical impact or mechanical energy (moving parts)	[location]		
Mechanical properties (Sharp, rough, slippery)	[location]		
Vibration	[location]		
Vehicles and Means of Transport	[location]		
Noise			
Frequency	[frequency],[Hz]		
Intensity			
Physical			
Confined spaces	[location]		
High workplaces	[location]		
Access to high workplaces	[location]		
Obstructions in passageways	[location]		
Manual handling	[location]		
Poor ergonomics	[location]		

Hazard identification:

Average electrical power requirements (excluding fixed ISOLDE-installation mentioned above): [make a rough estimate of the total power consumption of the additional equipment used in the experiment]: ... kW